



**UniMAP**

055675  
rb

f TN693

M3N974

2012

**Microstructure and Corrosion Protection of  
Magnesium alloy in Conversion Coating for  
Manufacturing Application**

by

**NURUL FARAH WAHIDA BINTI MOHD SIDIK  
(1130510580)**

A thesis submitted in fulfillment of the requirements for the degree of  
Master of Science

**School of Manufacturing Engineering  
UNIVERSITI MALAYSIA PERLIS**

2012

**GRADUATE SCHOOL**

**UNIVERSITI MALAYSIA PERLIS**

**PERMISSION TO USE**

In presenting this thesis in fulfillment of a post graduate degree from Universiti Malaysia Perlis, I agree that permission for copying of this thesis in any manner, in whole or in part, for scholarly purposes may be granted by my supervisor or, in their absence by Dean of the Graduate School. It is understood that any copying or publications or use of this thesis or parts thereof for financial gain shall not be allowed without my written permission. It is also understood that due to recognition shall be given to me and to Universiti Malaysia Perlis for any scholarly use which may be made of any materials from my thesis.

Request for permission to copy or make other use of material in whole or in part of this thesis are to be addressed to:

**Dean Centre for Graduate Studies (CGS)**

**Universiti Malaysia Perlis**

**No. 112 & 114 (First Floor)**

**Taman Pertiwi Indah, Jalan Kangar-Alor Setar**

**Seriab, 01000 Kangar,**

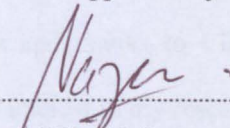
**Perlis**

**Malaysia**

## APPROVAL AND DECLARATION SHEET

This thesis entitled Microstructure and Corrosion Protection of Magnesium alloy in Conversion Coating for Manufacturing Application was prepared and submitted by Nurul Farah Wahida Binti Mohd Sidik (Matrix Number: 1130510580) and has be found satisfactory in terms of scope, quality and presentation as partial fulfillment of the requirement for the award of degree of Master Science (Manufacturing Engineering) in Universiti Malaysia Perlis (UniMAP).

Checked and Approved by

by   
.....  
(En Mohd Zamzuri Bin Mohammad Zain)

School of Manufacturing Engineering

Universiti Malaysia Perlis

(Date: 16/5/2013 )

School of Manufacturing Engineering

Universiti Malaysia Perlis

2012

## ACKNOWLEDGEMENTS

Alhamdulillah, thanks to God Almighty for His blesses and strength that He has gave to me to finish my research. Even though I had faced many challenges during my research that make my research progression becomes low as well as my motivation. However, thanks to Allah S.W.T and Prophet Muhammad S.A.W, finally I got strength to move on and capable to finish my research with the support from others.

First of all, most my gratitude goes to my supervisor and co-supervisor, En Mohd Zamzuri Mohammad Zain and Dr Mohd Nazree Derman, who providing valuable guidance and suggestions on this work. Their supervisions and support truly help me to keep this research going smoothness and thanks to Cik Siti Norbahiyah Mohamad Badari for her concerned and showing interest in my research and also offering valuable suggestion during various stages of my studies. My special thanks also go to the Dean of School Manufacturing Engineering, Dr Khairul Azwan Ismail for his valuable support.

My grateful thanks also go to the Technical Staff of Universiti Malaysia Perlis at Ulu Pauh Laboratory, En Mazlan, En Jasmin, En Suhelmi, En Fairuz and also Technical Staff of Material Laboratory at Taman Muhibbah, En Wan Mohd Arif who had become the back bone of my experimental work. Without their tremendous technical support, I can't manage to complete this project on the time.

I would like to give my sincere appreciations to my research team, Shalieza, Chye Lih, Naim and Fadzilah, who has offered their help during my laboratory session. I also acknowledge En Murizam and En Hafiz from School of Material for helping me in using X-Ray Diffraction software (XRD). I would also like to thank a long list of

people for many enjoyable scientific discussions and personal conversations-Khalid, Liyana, Faizal, Hafiz, Anwar, Kak Emma, Puan Kartini, Pn Marina and every else former and current of Manufacturing group members. Their time, expertise and warm friendship were very much appreciated.

I wish to thank Fundamental Research Grant and My Brain15 by the Ministry of High Education for financially supported during my research work starting from July 2011 until July 2012.

Finally, I want to express my appreciations to my beloved family- Papa, Mama, Syafiq, Amirah, Nasuha, Nadhirah, Lutfi and not forgetting my fiancée Muhamad Sharif for their love and encouragement. Thank you very much for supporting me every step of the way.

## TABLE OF CONTENTS

	<b>PAGES</b>
<b>DECLARATION OF THESIS</b>	ii
<b>COPYRIGHT</b>	iii
<b>APPROVAL AND DECLARATION SHEET</b>	iv
<b>ACKNOWLEDGEMENT</b>	v
<b>TABLE OF CONTENTS</b>	vii
<b>LIST OF TABLES</b>	xi
<b>LIST OF FIGURES</b>	xiii
<b>LIST OF ABBREVIATIONS</b>	xvi
<b>LIST OF SYMBOLS</b>	xxvii
<b>ABSTRACT</b>	xxviii
<b>ABSTRAK</b>	xxix
<b>CHAPTER 1 BACKGROUND</b>	
1.1 Introduction	1
1.2 AZ91D Magnesium alloy	1
1.3 Conversion Coating	3

1.4	Problem Statement	4
1.5	Research Objective	5
1.6	Research scope	5
1.7	Organization of Dissertation	7

## **CHAPTER 2 LITERATURE REVIEW**

2.1	Introduction	8
2.2	History of Magnesium Alloys	9
2.3	Alloy development	9
2.4	Definition of corrosion	11
	2.4.1 Types of corrosion	12
	2.4.1.1 Galvanic corrosion	12
	2.4.1.2 Pitting corrosion	13
	2.4.1.3 Crevice corrosion	14
	2.4.1.4 Intergranular corrosion	14
	2.4.1.5 Filiform corrosion	15
	2.4.1.6 Stress corrosion cracking (SCC)	16
2.5	Definition of coating	16
2.5.1	Coating Techniques	17
	2.5.1.1 Gas-phase deposition processes	18
	2.5.1.1.1 Physical Vapor Deposition (PVD)	18
	2.5.1.1.2 Chemical Vapor Deposition (CVD)	18
	2.5.1.2 Electrochemical Plating	19

2.5.1.3	Anodizing	21
2.6	Beta Phase	22
2.7	Potentiodynamic Polarization Curve	23
2.8	Chapter Summary	25
<b>CHAPTER 3 RESEARCH METHODOLOGY</b>		
3.1	Introduction	26
3.2	Material and surface treatment preparation	27
3.3	Mounting	29
3.4	Conversion coating	30
3.5	Corrosion test	31
3.6	Evaluation of the coating film	32
3.6.1	Surface characterization	32
3.7	Electrochemical measurement	34
3.8	Chapter Summary	35
<b>CHAPTER 4 RESULT AND DISCUSSION</b>		
4.1	Introduction	36
4.2	Evaluation of Coating Film	36
4.2.1	Untreated sample	36
4.2.2	Effect of NaVO <sub>3</sub> concentration	39
4.2.2.1	La (NO <sub>3</sub> ) <sub>3</sub> + NaVO <sub>3</sub>	39
4.2.2.2	Mg (NO <sub>3</sub> ) <sub>2</sub> + NaVO <sub>3</sub>	43

4.2.2.3 La (NO <sub>3</sub> ) <sub>3</sub> + Mg (NO <sub>3</sub> ) <sub>2</sub> + NaVO <sub>3</sub>	48
4.2.3 Effect of treatment time	52
4.2.3.1 La (NO <sub>3</sub> ) <sub>3</sub> + NaVO <sub>3</sub>	52
4.2.3.2 Mg (NO <sub>3</sub> ) <sub>2</sub> + NaVO <sub>3</sub>	56
4.2.3.3 La (NO <sub>3</sub> ) <sub>3</sub> + Mg (NO <sub>3</sub> ) <sub>2</sub> + NaVO <sub>3</sub>	60
4.2.4 Effect of pH	64
4.2.4.1 La (NO <sub>3</sub> ) <sub>3</sub> + NaVO <sub>3</sub>	64
4.2.4.2 Mg (NO <sub>3</sub> ) <sub>2</sub> + NaVO <sub>3</sub>	67
4.2.4.3 La (NO <sub>3</sub> ) <sub>3</sub> + Mg (NO <sub>3</sub> ) <sub>2</sub> + NaVO <sub>3</sub>	71
4.3 Corrosion Behavior	74
4.3.1 Untreated sample	74
4.3.2 Corrosion Behavior of different NaVO <sub>3</sub> concentration	75
4.3.2.1 La (NO <sub>3</sub> ) <sub>3</sub> + NaVO <sub>3</sub>	75
4.3.2.2 Mg (NO <sub>3</sub> ) <sub>2</sub> + NaVO <sub>3</sub>	84
4.3.2.3 La (NO <sub>3</sub> ) <sub>3</sub> + Mg (NO <sub>3</sub> ) <sub>2</sub> + NaVO <sub>3</sub>	91
4.3.3 Corrosion Behavior of treatment time	97
4.3.3.1 La (NO <sub>3</sub> ) <sub>3</sub> + NaVO <sub>3</sub>	97
4.3.3.2 Mg (NO <sub>3</sub> ) <sub>2</sub> + NaVO <sub>3</sub>	103
4.3.3.3 La (NO <sub>3</sub> ) <sub>3</sub> + Mg (NO <sub>3</sub> ) <sub>2</sub> + NaVO <sub>3</sub>	109

4.3.4	Corrosion Behavior of pH	116
4.3.4.1	La (NO <sub>3</sub> ) <sub>3</sub> + NaVO <sub>3</sub>	116
4.3.4.2	Mg (NO <sub>3</sub> ) <sub>2</sub> + NaVO <sub>3</sub>	121
4.3.4.3	La (NO <sub>3</sub> ) <sub>3</sub> + Mg (NO <sub>3</sub> ) <sub>2</sub> + NaVO <sub>3</sub>	125
4.4	Chapter Summary	130

## **CHAPTER 5 CONCLUSIONS AND RECOMMENDATION FOR FUTURE WORKS**

5.1	Introduction	131
5.2	Conclusion	131
5.3	Recommendation for Future Works	133

## **REFERENCES**

### **APPENDIX A: Journal Publications**

### **APPENDIX B: Conference Proceeding Publications**

### **APPENDIX C: Posters**

## LIST OF TABLES

TABLES	TITLE	PAGES
Table 3.1	Chemical composition of AZ91D magnesium alloy (wt. %)	28
Table 4.1	EDS result of different region examination of the conversion film formed in $\text{La}(\text{NO}_3)_3$ base solutions with different concentration of $\text{NaVO}_3$	42
Table 4.2	EDS result of different region examination of the conversion film formed in $\text{Mg}(\text{NO}_3)_2$ base solutions with different concentration of $\text{NaVO}_3$	47
Table 4.3	EDS result of different region examination of the conversion film formed in $\text{La}(\text{NO}_3)_3 + \text{Mg}(\text{NO}_3)_2$ base solutions with different concentration of $\text{NaVO}_3$	52
Table 4.4	EDS result of different region examination of the conversion film formed in $\text{La}(\text{NO}_3)_3$ base solutions with different treatment time	55
Table 4.5	EDS result of different region examination of the conversion film formed in $\text{Mg}(\text{NO}_3)_2$ base solutions with different treatment time	59
Table 4.6	EDS result of different region examination of the conversion film formed in $\text{La}(\text{NO}_3)_3 + \text{Mg}(\text{NO}_3)_2$ base solution with different treatment time	63

Table 4.7	EDS result of different region examination of the conversion film formed in La (NO <sub>3</sub> ) <sub>3</sub> base solutions with different pH	66
Table 4.8	EDS result of different region examination of the conversion film formed in Mg (NO <sub>3</sub> ) <sub>2</sub> base solutions with different pH	68
Table 4.9	EDS result of different region examination of the conversion film formed in La (NO <sub>3</sub> ) <sub>2</sub> + Mg (NO <sub>3</sub> ) <sub>2</sub> base solution with different pH	73
Table 4.10	Parameter values of potentiodynamic polarization curve of AZ91D Mg alloy in La (NO <sub>3</sub> ) <sub>3</sub> base solution with various concentration of NaVO <sub>3</sub>	81
Table 4.11	Parameter values of potentiodynamic polarization curve of AZ91D Mg alloy in Mg (NO <sub>3</sub> ) <sub>2</sub> base solution with various concentration of NaVO <sub>3</sub>	88
Table 4.12	Parameter values of potentiodynamic polarization curve of AZ91D Mg alloy in La (NO <sub>3</sub> ) <sub>3</sub> +Mg (NO <sub>3</sub> ) <sub>2</sub> base solution with various concentration of NaVO <sub>3</sub>	94
Table 4.13	Parameter values of potentiodynamic polarization curve of AZ91D Mg alloy in Mg (NO <sub>3</sub> ) <sub>2</sub> base solution with different treatment time	106

## LIST OF FIGURES

FIGURE	TITLE	PAGES
Figure 2.1	Capacity primary magnesium	10
Figure 2.2	Magnesium apportioned to metallurgical applications	11
Figure 2.3	Directions of alloy development	11
Figure 2.4	Galvanic corrosion	13
Figure 2.5	Pitting corrosion	13
Figure 2.6	Crevice corrosion	14
Figure 2.7	Intergranular corrosion	15
Figure 2.8	Filiform corrosion	15
Figure 2.9	Stress corrosion cracking	16
Figure 2.10	A classification scheme of coating techniques	17
Figure 3.1	Flow chart methodology of experimental work in evaluation of coating film	27
Figure 3.2	(a) Magnesium alloy (before), (b) Magnesium alloy (after)	28
Figure 3.3	Epofix Resin and Hardener	29
Figure 3.4	Grinding and Polishing machine	29
Figure 3.5	Flow chart methodology of corrosion test	32
Figure 3.6	Optical Microscope at UniMAP's Ulu Pauh Laboratory	33
Figure 3.7	Scanning Electron Microscope (SEM) at UniMAP's Ulu Pauh Laboratory	33

Figure 3.8	Schematic illustration of potentiodynamic polarization curve at UniMAP'S Nano Institute	34
Figure 4.1	Optical micrograph image of the microstructure of untreated sample AZ91D magnesium alloy, the microstructure typically consisting of a matrix of primarily $\alpha$ -phase grains surrounded by and $\beta$ -phase ( $Mg_{17}Al_{12}$ )	37
Figure 4.2	SEM backscattered image of the microstructure of untreated sample AZ91D magnesium alloy, the microstructure typically consisting of a matrix of primarily $\alpha$ -phase grains surrounded by eutectic $\alpha/\beta$ -constituent and $\beta$ -phase ( $Mg_{17}Al_{12}$ ). The $\alpha/\beta$ -constituent and $\beta$ -phase can be seen as the light gray and white areas, respectively	38
Figure 4.3	Optical micrograph of vanadia treated formed in electrolytes containing (a) $La(NO_3)_3$ base solutions and various concentrations of $NaVO_3$ , (b) 1g/l; (c) 3g/l; (d) 5g/l and (e) 7g/l respectively	39
Figure 4.4	Surface morphology of vanadia treated formed in electrolytes containing (a) $La(NO_3)_3$ base solutions and various concentrations of $NaVO_3$ , (b) 1g/l; (c) 3g/l; (d) 5g/l and (e) 7g/l respectively	40
Figure 4.5	Cross-sectional microstructure of the conversion coating on AZ91D Mg alloy treated with a) $La(NO_3)_3$ base solutions and b) 5 g/l additional of $NaVO_3$	41
Figure 4.6	Optical micrograph of vanadia treated formed in electrolytes containing (a) $Mg(NO_3)_2$ base solutions and various concentrations of $NaVO_3$ , (b) 1g/l; (c) 3g/l; (d) 5g/l and (e) 7g/l respectively	43

Figure 4.7	Surface morphology of vanadia treated formed in electrolytes containing (a) Mg (NO <sub>3</sub> ) <sub>2</sub> base solutions and various concentrations of NaVO <sub>3</sub> , (b) 1g/l; (c) 3g/l; (d) 5g/l and (e) 7g/l respectively	44
Figure 4.8	Cross-sectional microstructure of the conversion coating on AZ91D Mg alloy treated with a) Mg (NO <sub>3</sub> ) <sub>2</sub> base solutions and b) 5 g/l additional of NaVO <sub>3</sub>	46
Figure 4.9	XRD patterns for samples treated in Mg (NO <sub>3</sub> ) <sub>2</sub> base solutions with additional of 5 g/l NaVO <sub>3</sub>	48
Figure 4.10	Optical micrograph of vanadia treated formed in electrolytes containing (a) La (NO <sub>3</sub> ) <sub>3</sub> + Mg (NO <sub>3</sub> ) <sub>2</sub> base solutions and various concentrations Of NaVO <sub>3</sub> , (b) 1g/l; (c) 3g/l; and (d) 5g/l respectively	49
Figure 4.11	Surface morphology of vanadia treated formed in electrolytes containing (a) La (NO <sub>3</sub> ) <sub>3</sub> + Mg (NO <sub>3</sub> ) <sub>2</sub> base solutions and various concentrations Of NaVO <sub>3</sub> , (b) 1g/l; (c) 3g/l; and (d) 5g/l respectively	50
Figure 4.12	Cross-sectional microstructure of the conversion coating on AZ91D Mg alloy treated with a) 1 g/l additional of NaVO <sub>3</sub> and b) 5 g/l additional of NaVO <sub>3</sub> in La (NO <sub>3</sub> ) <sub>3</sub> + Mg (NO <sub>3</sub> ) <sub>2</sub> base solutions	51
Figure 4.13	Optical micrograph of vanadia treated formed in La (NO <sub>3</sub> ) <sub>3</sub> base solutions containing additional of 5 g/l NaVO <sub>3</sub> for (a) 10 min; (b) 15 min; (c) 20 min; (d) 25 min; (e) 30 min and (f) 35 min respectively	53
Figure 4.14	SEM morphology of samples treated in La (NO <sub>3</sub> ) <sub>3</sub> base solutions with 5 g/l NaVO <sub>3</sub> (a) 10 min (b) 30 min respectively	54

Figure 4.15	Cross-sectional microstructure of the conversion coating on AZ91D Mg alloy treated with a) 10 min and b) 30 min in La (NO <sub>3</sub> ) <sub>3</sub> base solutions	54
Figure 4.16	Optical micrograph of vanadia treated formed in Mg (NO <sub>3</sub> ) <sub>2</sub> base solutions containing 5 g/l NaVO <sub>3</sub> for (a) 10 min; (b) 15 min; (c) 20 min; (d) 25 min; (e) 30 min and (f) 35 min respectively	56
Figure 4.17	SEM morphology of samples treated in Mg (NO <sub>3</sub> ) <sub>2</sub> base solutions with 5 g/l NaVO <sub>3</sub> (a) 20 min (b) 30 min respectively	58
Figure 4.18	Cross-sectional microstructure of the conversion coating on AZ91D Mg alloy treated with a) 20 min and b) 30 min in Mg (NO <sub>3</sub> ) <sub>2</sub> base solutions	58
Figure 4.19	XRD patterns for samples treated in Mg (NO <sub>3</sub> ) <sub>2</sub> solutions with additional of 5 g/l NaVO <sub>3</sub> at 30 min	60
Figure 4.20	Optical micrograph of vanadia treated formed in La (NO <sub>3</sub> ) <sub>3</sub> + Mg (NO <sub>3</sub> ) <sub>2</sub> base solutions containing 5 g/l NaVO <sub>3</sub> for (a) 10 min; (b) 15 min; (c) 20 min; (d) 25 min; (e) 30 min and (f) 35 min respectively	61
Figure 4.21	SEM morphology of samples treated in La (NO <sub>3</sub> ) <sub>3</sub> + Mg (NO <sub>3</sub> ) <sub>2</sub> base solutions with 5 g/l NaVO <sub>3</sub> (a) 25 min (b) 35 min respectively	62
Figure 4.22	Cross-sectional microstructure of the conversion coating on AZ91D Mg alloy treated with a) 25 min and b) 35 min in La (NO <sub>3</sub> ) <sub>3</sub> + Mg (NO <sub>3</sub> ) <sub>2</sub> base solutions	62
Figure 4.23	Optical micrograph of vanadia treated formed in La (NO <sub>3</sub> ) <sub>3</sub> based solutions at different pH (a) 8.5; (b) 10.5 and (c) 12.5 respectively	64

Figure 4.24	SEM morphology of samples treated in $\text{La}(\text{NO}_3)_3$ base solutions with different pH (a) pH 8.5 (b) pH 12.5 respectively	65
Figure 4.25	Cross-sectional microstructure of the conversion coating on AZ91D Mg alloy treated with a) pH 8.5 and b) pH 12.5 in $\text{La}(\text{NO}_3)_3$ base solutions	65
Figure 4.26	Optical micrograph of vanadia treated formed in $\text{Mg}(\text{NO}_3)_2$ base solutions at different pH (a) 8.5; (b) 10.5 and (c) 12.5 respectively	67
Figure 4.27	SEM morphology of samples treated in $\text{Mg}(\text{NO}_3)_2$ base solutions with different pH (a) pH 8.5 (b) pH 12.5 respectively	68
Figure 4.28	Cross-sectional microstructure of the conversion coating on AZ91D Mg alloy treated with a) pH 8.5 and b) pH 12.5 in $\text{Mg}(\text{NO}_3)_2$ base solutions.	68
Figure 4.29	XRD patterns for samples treated in $\text{Mg}(\text{NO}_3)_2$ solutions with 8.5 pH	70
Figure 4.30	Optical micrograph of vanadia treated formed in $\text{La}(\text{NO}_3)_3 + \text{Mg}(\text{NO}_3)_2$ base solutions at different pH (a) 8.5; (b) 10.5 and (c) 12.5 respectively	71
Figure 4.31	SEM morphology of samples treated in $\text{La}(\text{NO}_3)_3 + \text{Mg}(\text{NO}_3)_2$ base solutions with different pH (a) pH 10.5 (b) pH 12.5 respectively	72
Figure 4.32	Cross-sectional microstructure of the conversion coating on AZ91D Mg alloy treated with a) pH 10.5 and b) pH 12.5 in $\text{La}(\text{NO}_3)_2 + \text{Mg}(\text{NO}_3)_2$ base solutions	73
Figure 4.33	Optical micrographs of conversion coatings for untreated sample	74

Figure 4.34	SEM for untreated sample	74
Figure 4.35	Visual inspection for vanadia treated for untreated sample after 72 hr corrosion in NaCl solutions	75
Figure 4.36	Corrosion rate of sample with conversion coating by immersion in La (NO <sub>3</sub> ) <sub>3</sub> base solutions at different concentration of NaVO <sub>3</sub> for 72hr in NaCl solutions	76
Figure 4.37	Optical micrograph of vanadia treated formed in electrolytes containing (a) La (NO <sub>3</sub> ) <sub>3</sub> various concentrations of NaVO <sub>3</sub> , (b) 1g/l; (c) 3g/l; (d) 5g/l and (e) 7g/l respectively	77
Figure 4.38	Surface morphology of vanadia treated formed in electrolytes containing (a) La (NO <sub>3</sub> ) <sub>3</sub> various concentrations of NaVO <sub>3</sub> , (b) 1g/l; (c) 3g/l; (d) 5g/l and (e) 7g/l respectively	79
Figure 4.39	The potentiodynamic polarization curve of untreated and sample treated in La (NO <sub>3</sub> ) <sub>3</sub> base solutions with different concentration of NaVO <sub>3</sub>	81
Figure 4.40	Visual inspection for vanadia treated in La (NO <sub>3</sub> ) <sub>3</sub> solutions (a) before corrosion and (b) after 72 hr in NaCl solutions	82
Figure 4.41	Visual inspection for vanadia treated with additional 1g/l NaVO <sub>3</sub> in La (NO <sub>3</sub> ) <sub>3</sub> solutions (a) before corrosion and (b) after 72 hr in NaCl solutions.	82
Figure 4.42	Visual inspection for vanadia treated with additional 3g/l NaVO <sub>3</sub> in La (NO <sub>3</sub> ) <sub>3</sub> solutions (a) before corrosion and (b) after 72 hr in NaCl solutions	83
Figure 4.43	Visual inspection for vanadia treated with additional 5g/l NaVO <sub>3</sub> in La (NO <sub>3</sub> ) <sub>3</sub> solutions (a) before corrosion and (b) after 72 hr in NaCl solutions	83

Figure 4.44	Visual inspection for vanadia treated with additional 7g/l NaVO <sub>3</sub> in La (NO <sub>3</sub> ) <sub>3</sub> solutions (a) before corrosion and (b) after 72 hr in NaCl solutions	83
Figure 4.45	Corrosion rate of sample with conversion coating by immersion in Mg (NO <sub>3</sub> ) <sub>2</sub> base solutions at different concentration of NaVO <sub>3</sub> for 72hr in NaCl solutions	84
Figure 4.46	Optical micrograph of vanadia treated formed in electrolytes containing (a) Mg (NO <sub>3</sub> ) <sub>2</sub> various concentrations Of NaVO <sub>3</sub> , (b) 1g/l; (c) 3g/l; (d) 5g/l and (e) 7g/l respectively	85
Figure 4.47	Surface morphology of vanadia treated formed in electrolytes containing (a) Mg (NO <sub>3</sub> ) <sub>2</sub> various concentrations Of NaVO <sub>3</sub> , (b) 1g/l; (c) 3g/l; (d) 5g/l (e) focus image on self-healing and (f) 7g/l respectively	86
Figure 4.48	The potentiodynamic polarization curve of untreated and sample treated in Mg (NO <sub>3</sub> ) <sub>2</sub> base solutions with different concentration of NaVO <sub>3</sub>	88
Figure 4.49	Visual inspection for vanadia treated in Mg (NO <sub>3</sub> ) <sub>2</sub> solutions (a) before corrosion and (b) after 72 hr in NaCl solutions.	89
Figure 4.50	Visual inspection for vanadia treated with additional 1g/l NaVO <sub>3</sub> in Mg (NO <sub>3</sub> ) <sub>2</sub> solutions (a) before corrosion and (b) after 72 hr in NaCl solutions	89
Figure 4.51	Visual inspection for vanadia treated with additional 3g/l NaVO <sub>3</sub> in Mg (NO <sub>3</sub> ) <sub>2</sub> solutions (a) before corrosion and (b) after 72 hr in NaCl solutions	90
Figure 4.52	Visual inspection for vanadia treated with additional 5g/l NaVO <sub>3</sub> in Mg (NO <sub>3</sub> ) <sub>2</sub> solutions (a) before corrosion and (b) after 72 hr in NaCl solutions	90

Figure 4.53	Visual inspection for vanadia treated with additional 7g/l NaVO <sub>3</sub> in Mg (NO <sub>3</sub> ) <sub>2</sub> solutions (a) before corrosion and (b) after 72 hr in NaCl solutions	90
Figure 4.54	Corrosion rate of sample with conversion coating by immersion in La (NO <sub>3</sub> ) <sub>3</sub> + Mg (NO <sub>3</sub> ) <sub>2</sub> base solution at different concentration of NaVO <sub>3</sub> for 72hr in NaCl solutions	91
Figure 4.55	Optical micrograph of vanadia treated formed in electrolytes containing (a) La (NO <sub>3</sub> ) <sub>3</sub> + Mg (NO <sub>3</sub> ) <sub>2</sub> various concentrations of NaVO <sub>3</sub> , (b) 1g/l; (c) 3g/l; and (d) 5g/l respectively	92
Figure 4.56	Surface morphology of vanadia treated formed in electrolytes containing (a) La (NO <sub>3</sub> ) <sub>3</sub> + Mg (NO <sub>3</sub> ) <sub>2</sub> various concentrations of NaVO <sub>3</sub> , (b) 1g/l; (c) 3g/l; and (d) 5g/l respectively	93
Figure 4.57	The potentiodynamic polarization curve of untreated and sample treated in La (NO <sub>3</sub> ) <sub>3</sub> +Mg (NO <sub>3</sub> ) <sub>2</sub> base solution with different concentration of NaVO <sub>3</sub>	94
Figure 4.58	Visual inspection for vanadia treated in La (NO <sub>3</sub> ) <sub>3</sub> + Mg (NO <sub>3</sub> ) <sub>2</sub> solutions (a) before corrosion and (b) after 72 hr in NaCl solutions	95
Figure 4.59	Visual inspection for vanadia treated for 1g/l NaVO <sub>3</sub> and La (NO <sub>3</sub> ) <sub>3</sub> + Mg (NO <sub>3</sub> ) <sub>2</sub> solutions (a) before corrosion and (b) after 72 hr in NaCl solutions	95
Figure 4.60	Visual inspection for vanadia treated with additional 3g/l NaVO <sub>3</sub> in La (NO <sub>3</sub> ) <sub>3</sub> + Mg (NO <sub>3</sub> ) <sub>2</sub> solutions (a) before corrosion and (b) after 72 hr in NaCl solutions	96

Figure 4.61	Visual inspection for vanadia treated with additional 5g/l NaVO <sub>3</sub> in La (NO <sub>3</sub> ) <sub>3</sub> + Mg (NO <sub>3</sub> ) <sub>2</sub> solutions (a) before corrosion and (b) after 72 hr in NaCl solutions	96
Figure 4.62	Corrosion rate of sample with conversion coating by immersion in La (NO <sub>3</sub> ) <sub>3</sub> base solutions with different treatment time for 72hr in NaCl solutions	97
Figure 4.63	Optical micrograph of vanadia treated formed in La (NO <sub>3</sub> ) <sub>3</sub> base solutions containing 5 g/l NaVO <sub>3</sub> for (a) 10 min; (b) 15 min; (c) 20 min; (d) 25 min; (e) 30 min and (f) 35 min respectively	98
Figure 4.64	SEM morphology of samples treated in La (NO <sub>3</sub> ) <sub>3</sub> base solutions with 5 g/l NaVO <sub>3</sub> after immersion in NaCl solutions (a) 10 min (b) 30 min respectively	99
Figure 4.65	The potentiodynamic polarization curve of untreated and sample treated in La (NO <sub>3</sub> ) <sub>3</sub> base solutions with different treatment time	100
Figure 4.66	Visual inspection for vanadia treated (5g/l) for 10 minutes in La (NO <sub>3</sub> ) <sub>3</sub> base solutions (a) before corrosion and (b) after 72 hr in NaCl solutions	101
Figure 4.67	Visual inspection for vanadia treated (5g/l) for 15 minutes in La (NO <sub>3</sub> ) <sub>3</sub> base solutions (a) before corrosion and (b) after 72 hr in NaCl solutions	101
Figure 4.68	Visual inspection for vanadia treated (5g/l) for 20 minutes in La (NO <sub>3</sub> ) <sub>3</sub> base solutions (a) before corrosion and (b) after 72 hr in NaCl solutions	101
Figure 4.69	Visual inspection for vanadia treated (5g/l) for 25 minutes in La (NO <sub>3</sub> ) <sub>3</sub> base solutions (a) before corrosion and (b) after 72 hr in NaCl solutions	102

Figure 4.70	Visual inspection for vanadia treated (5g/l) for 30 minutes in La (NO <sub>3</sub> ) <sub>3</sub> base solutions (a) before corrosion and (b) after 72 hr in NaCl solutions	102
Figure 4.71	Visual inspection for vanadia treated (5g/l) for 35 minutes in La (NO <sub>3</sub> ) <sub>3</sub> base solutions (a) before corrosion and (b) after 72 hr in NaCl solutions	103
Figure 4.72	Corrosion rate of sample with conversion coating by immersion in Mg (NO <sub>3</sub> ) <sub>2</sub> base solutions at different treatment time for 72hr in NaCl solutions	103
Figure 4.73	Optical micrograph of vanadia treated formed in Mg (NO <sub>3</sub> ) <sub>2</sub> base solutions containing 5 g/l NaVO <sub>3</sub> for (a) 10 min; (b) 15 min; (c) 20 min; (d) 25 min; (e) 30 min and (f) 35 min respectively	104
Figure 4.74	SEM morphology of samples treated in Mg (NO <sub>3</sub> ) <sub>2</sub> base solutions with 5 g/l NaVO <sub>3</sub> after immersion NaCl solutions (a) 20 min (b) 30 min respectively	105
Figure 4.75	The potentiodynamic polarization curve of untreated and sample treated in Mg (NO <sub>3</sub> ) <sub>2</sub> base solutions with different treatment time	106
Figure 4.76	Visual inspection for vanadia treated (5g/l) for 10 minutes in Mg (NO <sub>3</sub> ) <sub>2</sub> base solutions (a) before corrosion and (b) after 72 hr in NaCl solutions	107
Figure 4.77	Visual inspection for vanadia treated (5g/l) for 15 minutes in Mg (NO <sub>3</sub> ) <sub>2</sub> base solutions (a) before corrosion and (b) after 72 hr in NaCl solutions	107

Figure 4.78	Visual inspection for vanadia treated (5g/l) for 20 minutes in Mg (NO <sub>3</sub> ) <sub>2</sub> base solutions (a) before corrosion and (b) after 72 hr in NaCl solutions	108
Figure 4.79	Visual inspection for vanadia treated (5g/l) for 25 minutes in Mg (NO <sub>3</sub> ) <sub>2</sub> base solutions (a) before corrosion and (b) after 72 hr in NaCl solutions	108
Figure 4.80	Visual inspection for vanadia treated (5g/l) for 30 minutes in Mg (NO <sub>3</sub> ) <sub>2</sub> base solutions (a) before corrosion and (b) after 72 hr in NaCl solutions.	108
Figure 4.81	Visual inspection for vanadia treated (5g/l) for 35 minutes in Mg (NO <sub>3</sub> ) <sub>2</sub> base solutions (a) before corrosion and (b) after 72 hr in NaCl solutions	109
Figure 4.82	Corrosion rate of sample with conversion coating by immersion in La (NO <sub>3</sub> ) <sub>3</sub> +Mg (NO <sub>3</sub> ) <sub>2</sub> base solution with different treatment time for 72hr in NaCl solutions	110
Figure 4.83	Optical micrograph of vanadia treated formed in La (NO <sub>3</sub> ) <sub>3</sub> + Mg (NO <sub>3</sub> ) <sub>2</sub> base solutions containing 5 g/l NaVO <sub>3</sub> for (a) 10 min; (b) 15 min; (c) 20 min; (d) 25 min; (e) 30 min and (f) 35 min respectively	111
Figure 4.84	SEM morphology of samples treated in La (NO <sub>3</sub> ) <sub>3</sub> +Mg (NO <sub>3</sub> ) <sub>2</sub> base solutions with 5 g/l NaVO <sub>3</sub> after immersion in NaCl solutions (a) 25 min (b) 35 min respectively	112
Figure 4.85	The potentiodynamic polarization curve of untreated and sample treated in La (NO <sub>3</sub> ) <sub>3</sub> +Mg (NO <sub>3</sub> ) <sub>2</sub> base solution at different treatment time	113

Figure 4.86	Visual inspection for vanadia treated (5g/l) for 10 minutes in La (NO <sub>3</sub> ) <sub>3</sub> + Mg (NO <sub>3</sub> ) <sub>2</sub> base solutions (a) before corrosion and (b) after 72 hr in NaCl solutions	114
Figure 4.87	Visual inspection for vanadia treated (5g/l) for 15 minutes in La (NO <sub>3</sub> ) <sub>3</sub> + Mg (NO <sub>3</sub> ) <sub>2</sub> base solutions (a) before corrosion and (b) after 72 hr in NaCl solutions	114
Figure 4.88	Visual inspection for vanadia treated (5g/l) for 20 minutes in La (NO <sub>3</sub> ) <sub>3</sub> + Mg (NO <sub>3</sub> ) <sub>2</sub> base solutions (a) before corrosion and (b) after 72 hr in NaCl solutions	114
Figure 4.89	Visual inspection for vanadia treated (5g/l) for 25 minutes in La (NO <sub>3</sub> ) <sub>3</sub> + Mg (NO <sub>3</sub> ) <sub>2</sub> based solutions (a) before corrosion and (b) after 72 hr in NaCl solutions	115
Figure 4.90	Visual inspection for vanadia treated (5g/l) for 30 minutes in La (NO <sub>3</sub> ) <sub>3</sub> + Mg (NO <sub>3</sub> ) <sub>2</sub> base solutions (a) before corrosion and (b) after 72 hr in NaCl solutions	115
Figure 4.91	Visual inspection for vanadia treated (5g/l) for 35 minutes in La (NO <sub>3</sub> ) <sub>3</sub> + Mg (NO <sub>3</sub> ) <sub>2</sub> base solutions (a) before corrosion and (b) after 72 hr in NaCl solutions	115
Figure 4.92	Corrosion rate of sample with conversion coating by immersion in La (NO <sub>3</sub> ) <sub>3</sub> base solutions at different pH for 72hr in NaCl solution	116
Figure 4.93	Optical micrograph of La (NO <sub>3</sub> ) <sub>3</sub> base solution with additional of NaVO <sub>3</sub> coatings obtained in different pH: (a) 8.5; (b) 10.5; (c) 12.5	117
Figure 4.94	SEM morphology of samples treated in La (NO <sub>3</sub> ) <sub>3</sub> base solutions with 5 g/l NaVO <sub>3</sub> after immersion in NaCl solutions (a) 8.5 (b) 12.5 respectively	118